JOURNAL OF MATERIALS SCIENCE 12 (1977) 2475–2487

A Mössbauer study of the oxidation of Fe-Ni alloys at 535 and 635°C

D. A. CHANNING
Faculty of Technology, The Open University, Milton Keynes, Bucks, UK

M. J. GRAHAM
Division of Chemistry, National Research Council of Canada, Ottawa, Ontario, Canada

G. A. SWALLOW
Materials Division, CEGB, Berkeley Nuclear Laboratories, Berkeley, Glos, UK

Fe^{57} transmission Mössbauer spectroscopy, supported by metallography, SEM and X-ray diffraction analysis, has been employed to study the oxidation of Fe–Ni alloys at 535 and 635° C in 1 atm. of air. With increasing Ni content of the alloy, the composition of the scale changed and the oxidation rate decreased. For an alloy containing 0.9% Ni, the oxide scale produced at 535° C was Fe_3O_4 covered by a thin outer layer of α-Fe_2O_3, while at 635° C FeO was additionally present as a major phase. The scale formed on a 10% Ni alloy at both 535 and 635° C was similar to that observed for the 0.9% Ni alloy oxidized at 535° C (i.e. of Fe_3O_4 and α-Fe_2O_3), although the α-Fe_2O_3 layer tended to be relatively thicker. For a 49% Ni alloy, the scale at both 535 and 635° C comprised an inner layer of $Ni_xFe_{3-x}O_4$ (with $x \approx 0.5$, on average) and an outer layer of α-Fe_2O_3, of similar thickness. Finally, on an 83% Ni alloy oxidized at 635° C, the scale consisted of roughly equally thick layers of NiO (next to the metal) and $NiFe_2O_4$, and a thin outer covering of α-Fe_2O_3. The decrease in oxidation rate with increasing Ni content of the alloy is discussed briefly in relation to the changing composition of the scale and diffusion in the alloy.

1. Introduction

In previous studies, we have used the Mössbauer effect in Fe^{57} for the investigation of the oxidation of α-iron [1–4]. The technique was found to be valuable for identifying the oxides produced and for deriving quantitative information about their growth mechanisms.

In the present work, the Mössbauer technique has been applied to a study of the oxidation of Fe–Ni alloys. Two primary purposes were in mind: firstly, to provide knowledge on the oxidation behaviour of the Fe–Ni system at moderate temperatures, for which very little data have been published*; and, secondly, to help establish the value of the method for general application to corrosion research on iron alloys.

Specifically, we have employed Fe^{57} transmission Mössbauer spectroscopy, complemented by metallography, scanning electron microscopy (SEM) and X-ray diffraction analysis, to investigate oxide formation in air at temperatures of 535 and 635° C on Fe–Ni alloys containing 0.9% Ni, 10% Ni, 49% Ni and 83% Ni. Emphasis has been placed on oxide identification and scale composition, although information on overall oxidation rates of the alloys has also been obtained.

2. Experimental

2.1. Samples and oxidation treatment

The Fe–Ni alloys were foils $\approx 28\,\mu m$ thick. The impurity level was ~ 400 ppm (by weight), the main impurities being C, Nb and Co in the 0.9%

*For a general review of Fe–Ni oxidation data up to 1962, see Foley [5]. Additional data published since that time have been confined essentially to high temperatures (> 700° C).

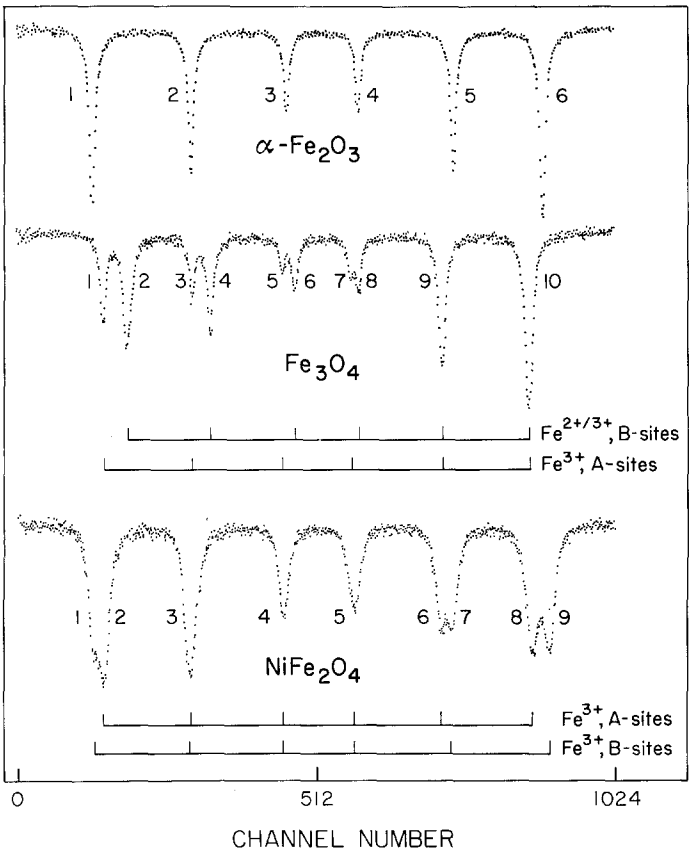

Figure 1 Room-temperature transmission Mössbauer spectra of α-Fe_2O_3, Fe_3O_4 and $NiFe_2O_4$.

and 10% Ni alloys, Mo and Ti in the 49% Ni alloy, and Co, Cr and Cu in the 83% Ni alloy*. For each alloy a series of specimens, about 10 mm x 10 mm square, were cut from the foils and oxidized in the as-received, cold-rolled state after degreasing in benzene or acetone. The oxidations were performed for a variety of times up to $\approx$ 400 h in laboratory air at a pressure of 1 atm. and with the temperature known to about $\pm 5^\circ$ C. The 0.9%, 10% and 49% Ni alloys were oxidized mainly at 535° C and the 83% Ni alloy mainly at 635° C. Following an oxidation, the sample was cooled rapidly to room temperature (in $\sim$ 5 min) and its Mössbauer spectrum determined.

2.2. Mössbauer spectroscopy

The spectra were recorded using conventional constant-acceleration spectrometers, either at Berkeley Nuclear Laboratories (BNL), or at the National Research Council of Canada (NRCC). Both instruments operated in the "time mode", the former with 400 channels for data storage and the latter with 1024 channels. The Mössbauer source was Co^{57} in Pd ($\approx$ 25 mCi at BNL, $\approx$ 70 mCi at NRCC). Deconvolution and intensity analysis of absorption lines were performed with the aid of a Dupont curve resolver (Type 310).

3. Background spectral data

The iron, or iron-containing, oxides that proved to be of prime interest in this study were α-Fe_2O_3 (hematite) and the inverse spinels Fe_3O_4 (magnetite) and $Ni_xFe_{3-x}O_4$ with $0 < x \leqslant 1$ (nickel ferrite). Before presenting our results, it will be helpful to review briefly the room-temperature spectral characteristics of these oxides and also those of the Fe–Ni alloy system.

3.1. Oxides

The spectra of α-Fe_2O_3, Fe_3O_4 and $NiFe_2O_4$ ($Ni_xFe_{3-x}O_4$ for $x = 1$) are shown in Fig. 1 with resolved peaks numbered 1, 2, 3, etc. in the order of increasing Doppler velocity. These spectra were recorded on high-purity powders ($\approx$ 15 mg cm^{-2}), the nickel ferrite being taken from a pressed pellet of thoroughly mixed NiO and α-Fe_2O_3 (in correct

*Our alloy compositions are in at. %.

proportions) which had been fired at 1000° C in air to produce the single-phase spinel.

Hematite shows as a single (Zeeman) pattern of six peaks whose separation corresponds to an internal (hyperfine) magnetic field, H_i, at the Fe nucleus of 517 kOe [6, 7].

The ten-peak spectrum for magnetite arises from two, partially-resolved six-line patterns, A and B. Pattern A, of greater splitting ($H_i = 492$ kOe), is due to Fe^{3+} ions at the tetrahedral interstices (A-sites), while B (with $H_i = 461$ kOe) is due to both Fe^{2+} and Fe^{3+} ions at the octahedral interstices (B-sites) [8–11]. The octahedral Fe^{2+} and Fe^{3+} are not spectrally distinguishable because of the rapid exchange of electrons, $Fe^{2+} \rightleftarrows Fe^{3+}$, which occurs between these ions; the observed absorption is an average of the spectra expected separately for the two ion species. Referring to the intensities (absorption line areas) of the A and B patterns as I_A and I_B, respectively, then $I_B/I_A \approx 1.88$ [12]*.

It may be assumed that nickel ferrite is derived from Fe_3O_4 by substitution of octahedral Fe^{2+} by Ni^{2+}. The cation distribution can thus be expressed by the formula

$$(Fe^{3+})_A\,(Ni_x^{2+}\,Fe_{1-x}^{2+}Fe^{3+})_B O_4$$

Relative to Fe_3O_4, the main obvious effect in the Mössbauer spectrum of replacing Fe^{2+} by Ni^{2+}, for $x \lesssim 0.6$, is to reduce the intensity I_B, with an accompanying increase in B pattern line-width, and to increase the intensity I_A [10, 11, 13]. The reduction in I_B does not occur simply because of the smaller number of B-site Fe^{2+} ions. The decrease also arises because the presence of Ni^{2+} prevents some of the octahedral Fe^{3+} from participating in the $Fe^{2+} \rightleftarrows Fe^{3+}$ interchange and consequently from contributing to the B pattern. These B-site Fe^{3+} ions, instead, produce a six-line spectrum which is directly superimposed on that due to the A-site Fe^{3+} ions and this gives rise to the increase in I_A. For x values of 0.2, 0.4 and 0.6, observed I_B/I_A ratios are respectively ≈ 1.46, 1.25 and 0.5 [11, 13]. From the I_B/I_A value and also from the enhanced B pattern line-width of the nickel-containing spinel, it is readily possible to distinguish between Fe_3O_4 and nickel ferrite of composition corresponding to $x = 0.1$ and it may be feasible to make the distinction with x as low as 0.05. In deriving I_B/I_A for the composite A and B spectrum use may be made of the fact that $I_B/I_A = I_2/I_1$ where I_1 is the intensity of peak 1 (the first line of the A pattern) and I_2 is the intensity of peak 2 (the first line of the B pattern).

As x increases beyond ≈ 0.6, the restriction imposed by Ni^{2+} on the electron exchange between B-site Fe ions leads to a second type of octahedral Fe^{3+} ion which is not involved in the exchange process [13]. These Fe^{3+} ions give rise to a third partially resolved six-line pattern which is of increased splitting ($H_i \approx 530$ kOe). This pattern is characteristic of octahedral Fe, all of which is Fe^{3+}, in $NiFe_2O_4$ and its intensity increases with increasing x, representing $\approx 1/6$ of the total absorption at $x = 0.8$ [13].

Finally, as the composition $NiFe_2O_4$ is approached, the spectrum returns to two overlapping sextets. These are of nearly equal intensity, the first being the A pattern, as in Fe_3O_4 due to the A-site Fe^{3+} ions, and the second with the larger splitting being due to the B-site Fe^{3+} ions [10, 13, 14].

3.2. Fe–Ni alloys

The Fe–Ni equilibrium diagram shows a fairly wide two-phase region, $\alpha(bcc) + \gamma(fcc)$, which increases in width with decreasing temperature. At the two oxidation temperatures used in the present work, 635 and 535° C, the α boundary compositions are respectively $\approx 3\%$ and 5% Ni, and the γ boundary compositions are correspondingly $\approx 14\%$ and 24% Ni [15].

At room temperature, the observed phases will be metastable and dependent upon both alloy composition and prior heat-treatment. Of present interest, alloys containing $\lesssim 25\%$ Ni which are cooled (at ordinary and fast rates) from temperatures above 500° C will tend to be solely bcc (γ-phase transforming martensitically to α-phase), while alloys with $\gtrsim 30\%$ Ni will tend to be solely fcc [15].

Except for the fcc phase containing around 30% Ni, both bcc and fcc phases are magnetically ordered at room temperature, and so six-line spectra are generally produced. The degree of splitting is determined by the crystal structure and Ni-content as reflected by the variation of H_i shown in Fig. 2 [16]. For the bcc structure the splitting

*Strictly, $I_B/I_A \approx 1.88$ applies only for extremely thin absorbers. In practice, because of thickness effects, the observed ratio is likely to extend down to ≈ 1.80.

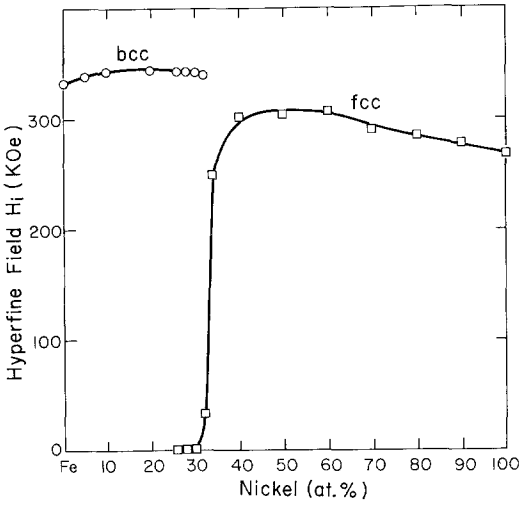

Figure 2 Hyperfine magnetic field, H_i, at the Fe^{57} nucleus in Fe–Ni alloys at room temperature (after Johnson *et al.* [16]).

varies slowly, passing through a maximum at $\approx 20\%$ Ni. In contrast, the variation for the f c c structure is quite marked, with the splitting falling dramatically below $\approx 40\%$ Ni. At 30% Ni or less, corresponding to the paramagnetic alloys, $H_i = 0$, and the spectrum reduces simply to a single line.

4. Results

Representative spectra for the 0.9%, 10% and 49% Ni alloys oxidized at 535° C, and for the 83% Ni alloy oxidised at 635° C are shown in Figs. 3, 5, 7 and 11, respectively. The stick diagrams locate the peak positions of α-Fe_2O_3, Fe_3O_4 and $NiFe_2O_4$, as appropriate, and also of the unoxidized Fe–Ni alloy. The spectra for the unoxidized metals show single patterns indicative of single-phase structure: b c c for the 0.9% and 10% Ni alloys; f c c for the 49% and 83% Ni alloys.

4.1. 0.9% Ni alloy

In view of the low Ni-content, the oxide phases expected and produced by the oxidation of specimens of this alloy at 535° C were those characteristic of the oxidation of pure iron at this temperature, i.e. magnetite and hematite. That the spinel observed at all stages of oxidation was indeed essentially Fe_3O_4 was evident from the relative intensities of the A and B spectral patterns (and from the lack of broadening of the B pattern linewidths). In Fig. 3, this is best seen via the first two peaks of the spinel spectrum and intensity analysis of these peaks gives an I_B/I_A ratio which remained at the value 1.8 ± 0.1.

The course of oxidation with time is followed conveniently in Fig. 3 via peaks 10 of Fe_3O_4 and 6 of α-Fe_2O_3, while the accompanying decrease of Fe in the alloy may be followed by peak 1 of the alloy pattern. Noting that the ratio of intensities of these particular peaks gives approximately the

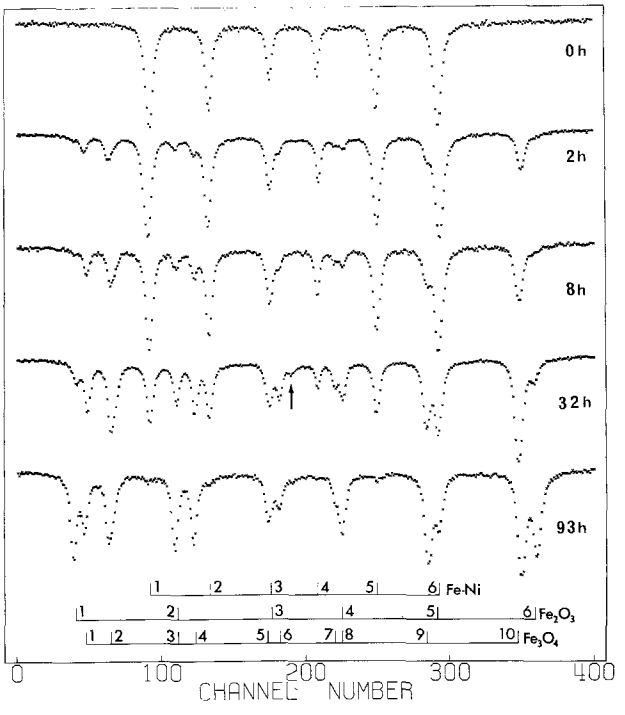

Figure 3 Room-temperature transmission Mössbauer spectra of $\approx 28\,\mu$m thick samples of Fe–0.9% Ni alloy oxidized at 535° C for the times indicated. The arrow on the 32 h spectrum locates the weak peak attributed to paramagnetic f c c alloy.

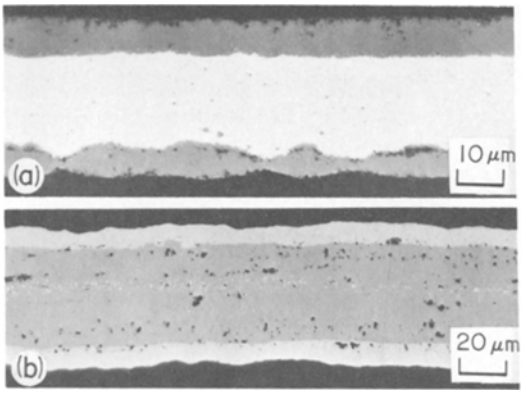

Figure 4 Metallographic sections of the Fe–0.9% Ni samples oxidized at 535° C: (a) 2 h, (b) 93 h.

relative amounts of Fe bound up respectively in the three components*, it is evident that the scale is mainly magnetite in the presence of a ready supply of Fe from the alloy. This applies in the spectra of Fig. 3 for oxidation periods up to 32 h, by which time ≈ 30% of the original Fe remains unoxidized. With further oxidation and eventual reaction of all Fe, α-Fe_2O_3 grows at the expense of Fe_3O_4. In the 93 h spectrum, the absorption from metallic Fe is only just discernible and α-Fe_2O_3 represents ≈ 35% of the scale.

The spectral pattern due to the b c c alloy is not detectably altered with increasing oxidation times as a consequence of alloy composition changes. This observation is again not unexpected considering the slow variation of H_i with Ni concentration in the b c c phase. An indication of Ni enrichment of the metal did occur, nevertheless, for the sample oxidized for 32 h. Its spectrum reveals a very weak central peak which may be attributed to a trace of paramagnetic γ-phase that has not transformed to α-phase on cooling to room temperature.

Metallographic cross-sections on the samples oxidized for 2 and 93 h are given in Fig. 4. After 2 h, the magnetite is seen to be a fairly compact layer in good contact with the alloy, and a thin outer layer of hematite is evident (as was also the case in the Mössbauer spectrum). The section for 93 h oxidation illustrates the relatively thick α-Fe_2O_3 overgrowth and shows the small amount of residual alloy existing at this time to be a dispersed, central band of particles.

4.2. 10% Ni alloy

The general similarity of the spectra in Fig 5 for the 10% Ni samples oxidized at 535° C with those of Fig. 3 for the 0.9% Ni alloy will be apparent. As before, there is no discernible effect of Ni on the iron oxide phases produced, which were evidently hematite and magnetite for all times of oxidation. The I_B/I_A ratio for the spinel component continued to remain at 1.8 ± 0.1 (and there was no detectable broadening of the B pattern lines relative to the Fe_3O_4 phase). If Ni did enter the spinel lattice it follows from Section 3.1 that its average concentration was $\lesssim 3\%$ of the spinel cations. Metallography did not reveal NiO in the samples, and none was found by X-ray diffraction analysis on the most extensively oxidized sample. In this latter sample, oxidized for 239 h, no metallic Fe could be detected in the Mössbauer spectrum.

The absorption pattern due to the residual alloy in the spectra of Fig. 5 continues, with increasing oxidation times, to be characteristic of b c c structure and shows no obvious features due to composition changes occurring in the alloy. The only deviation from this arises in the 17 and 73 h spectra where the weak central peak indicates the presence of a small paramagnetic f c c component. That there is no clear indication of six-line absorption attributable to ferromagnetic f c c phase in the spectra of the more highly oxidized samples is perhaps a little surprising. Probably, this reflects strong enrichment of Ni in the outer region of the alloy as the oxide/metal interface advances into the sample.

Structural features of the scale after 17 and 239 h are shown in the metallographic and SEM sections in Fig. 6. These features appear to be similar to those observed for the 0.9% Ni alloy (Fig. 4), although the spinel/alloy interface with the 10% Ni alloy was considerably more ragged in all samples examined.

4.3. 49% Ni alloy

The spectra in Fig. 7 for the 49% Ni samples oxidized at 535° C differ quite considerably from those for the oxidized 0.9% and 10% Ni alloys, and reveal two marked changes in the composition of the scale. Firstly, α-Fe_2O_3 is now a major iron oxide at all times of oxidation. Secondly, the

*This follows for these spectra since (i) the peaks 10 of Fe_3O_4, 6 of α-Fe_2O_3, and 1 of the alloy may be taken to account for ≈ 1/4 of the total intensities due individually to the three components and (ii) the ratio of these total intensities is approximately equal to the ratio of the components' corresponding Fe-contents (see Channing and Graham [3], for example).

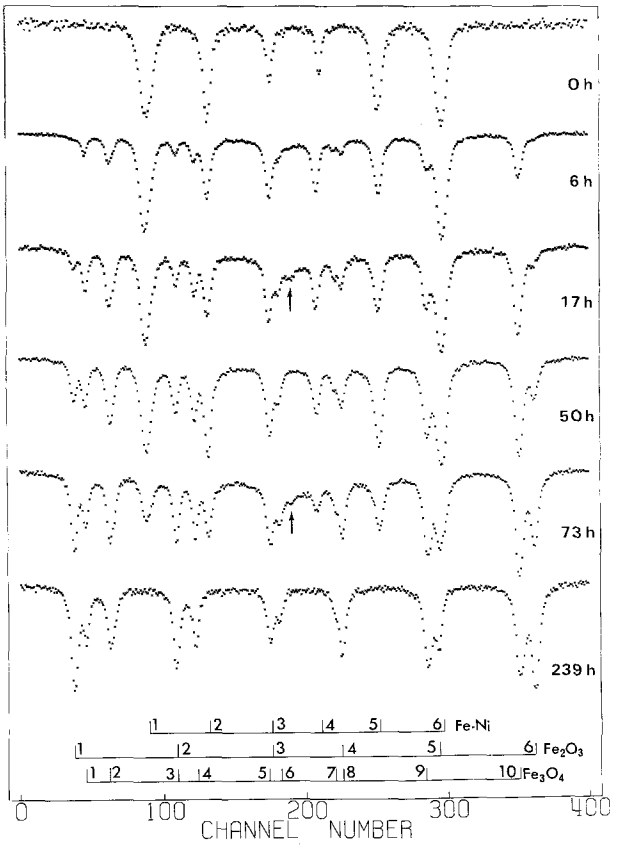

Figure 5 Room-temperature transmission Mössbauer spectra of $\approx 28\,\mu m$ thick samples of Fe–10% Ni alloy oxidized at 535° C for the times indicated. The arrows on the 17 and 73 h spectra locate the weak peak attributed to paramagnetic f c c alloy.

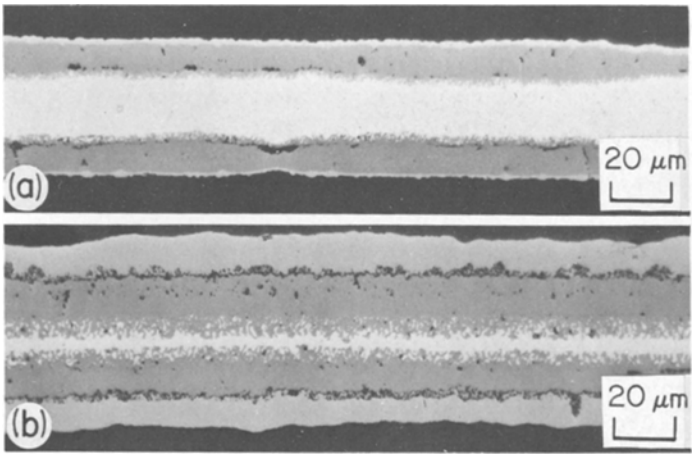

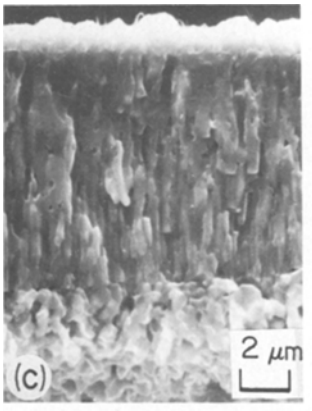

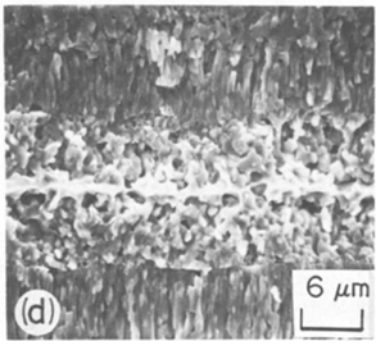

Figure 6 Metallographic and SEM sections of the Fe–10% Ni samples oxidized at 535° C: (a) and (c) 17 h; (b) and (d) 239 h. (c) is of only the oxide and (d) is of the central portion of the sample.

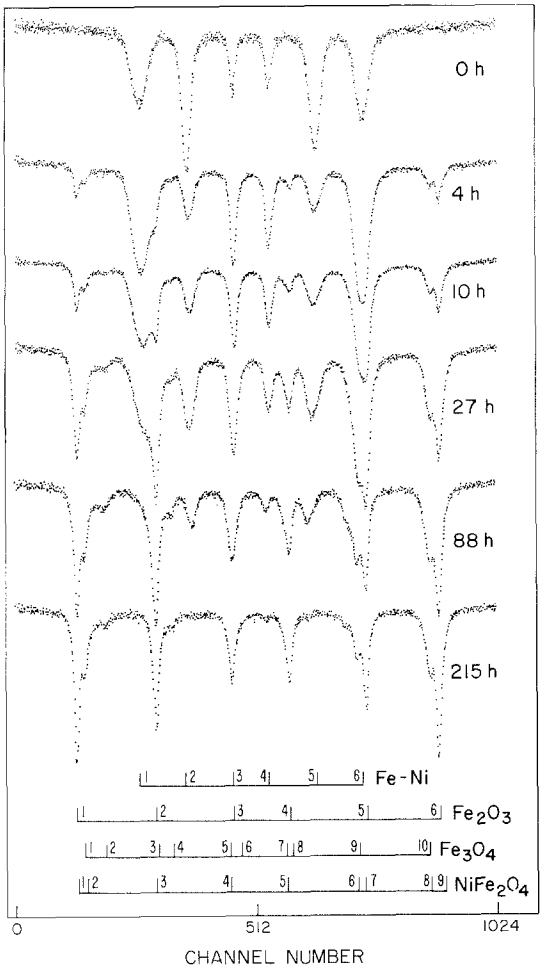

Figure 7 Room-temperature transmission Mössbauer spectra of $\approx 28\,\mu m$ thick samples of Fe–49% Ni alloy oxidized at 535° C for the times indicated.

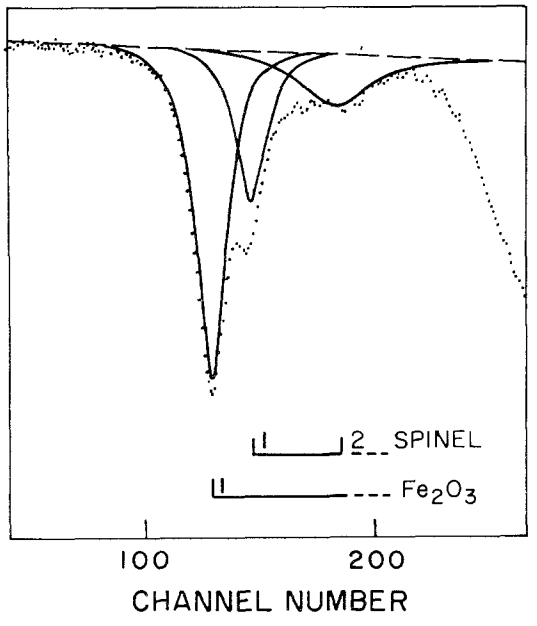

Figure 8 Deconvolution of the first two peaks due to the spinel on the Fe–49% Ni sample oxidized at 535° C for 27 h. Curve fitting assumed the peaks to be Lorentzian.

spinel is no longer simply Fe_3O_4 (or close to Fe_3O_4); appreciable Ni has entered the spinel lattice, as is evident from the strongly reduced B pattern intensity.

In the spectra corresponding to oxidations of 10 to 215 h, the spinel component appears to comprise only the A and B patterns and the I_B/I_A intensity ratio seems not to vary greatly which suggests a similar spinel composition in each case. Intensity analysis of the 27 and 215 h spectra, taken as representative, yields I_B/I_A values of 0.9 ± 0.1 and 0.8 ± 0.1, respectively. The analysis, as with the previous alloys, was based only upon the first two peaks due to the spinel and Fig. 8 shows the deconvolution of these peaks for the sample oxidized for 27 h. Reference to Section 3.1 suggests an average composition for the spinel in these samples which corresponds to $x \approx 0.5$, i.e. to the nickel ferrite $Ni_{0.5}Fe_{2.5}O_4$*.

Increasing Ni enrichment of the residual alloy with oxidation time is indicated in the spectra of Fig. 7. It shows by the steady decrease in splitting of the alloy pattern relative to the unoxidized material and is most easily seen by the displacement inwards of the peaks 2 and 5. After 10 h of oxidation, for example, the (average) internal field, H_i, has been reduced by $\approx 3\%$ and after 88 h the reduction is $\approx 9\%$. The diminished H_i value in the two cases would, from Fig. 2, be characteristic of (homogeneous) alloys containing $\approx 65\%$ Ni and $\approx 85\%$ Ni respectively†.

*For the 4 h spectrum, the counting statistics associated with the relatively weak oxide peaks are less favourable and it is more difficult to make an assessment of the spinel composition in this instance. It does appear, however, that the ferrite is richer in Ni than applies to the spinel formed on the more oxidized samples.

†It may be noticed in the spectra of Fig. 7 that the relative intensities of the six peaks in the alloy pattern may alter substantially after oxidation of the alloy. This is especially noticeable in the 4 and 10 h spectra (compare the intensities of peaks 4 and 5 of the alloy with those of the starting alloy) and is attributable to changes in the alloy's magnetic domain structure (see for instance Preston *et al.* [17]). The effect will also be highly evident in the oxidation results for the 83% Ni alloy (Fig. 11).

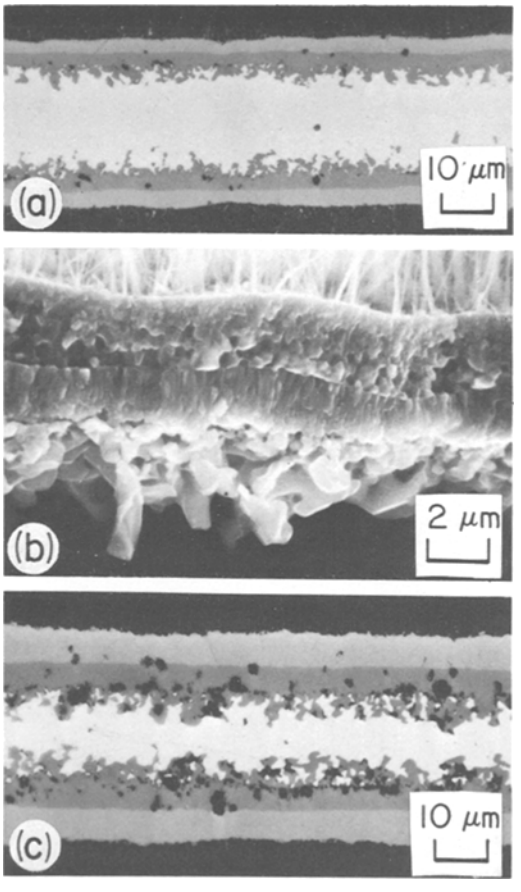

Figure 9 Metallographic and SEM sections of the Fe–49% Ni samples oxidized at 535° C: (a) and (b) 27 h; (c) 215 h. (b) is of the oxide only. The oxide comprises roughly equal amounts of spinel and α-Fe_2O_3.

Metallographic and SEM sections of the specimens oxidized 27 and 215 h are shown in Fig. 9. The relatively thick α-Fe_2O_3 layer is seen to be quite uniform and pore-free, and its exposed surface is densely covered by whiskers. The appearance of the spinel/alloy interface indicates the break-down of an unstable interface. NiO was not observed in any sections examined. Nor was it found by X-ray diffraction analysis of (i) the sample oxidized for 215 h (at which time only a very small amount of metallic Fe remained) and (ii) a sample oxidized (more extensively) for 385 h.

4.4. 83% Ni alloy

Preliminary experiments at 535° C on the 83% Ni alloy indicated that the oxidation rate was dramatically lower than observed with the less-rich alloys. As a consequence, useful transmission spectra could not be determined on samples oxidized at 535° C without using prohibitively long oxidation periods. Because of this the Mössbauer studies on the 83% Ni alloy were directed to samples oxidized at the higher temperature of 635° C.

As a check that the oxide phases produced by oxidation of this alloy at 635° C might be meaningfully compared with those formed by oxidation of the 0.9%, 10% and 49% Ni alloys at 535° C, one sample of each of these latter alloys was also examined after oxidation at 635° C. The resulting spectra, given in Fig. 10, show only one new feature in relation to the oxides produced: namely, the emergence of an asymmetric doublet due to wustite [18] which forms as an additional major phase on the 0.9% Ni alloy. Other features revealed by the three spectra, in particular whether

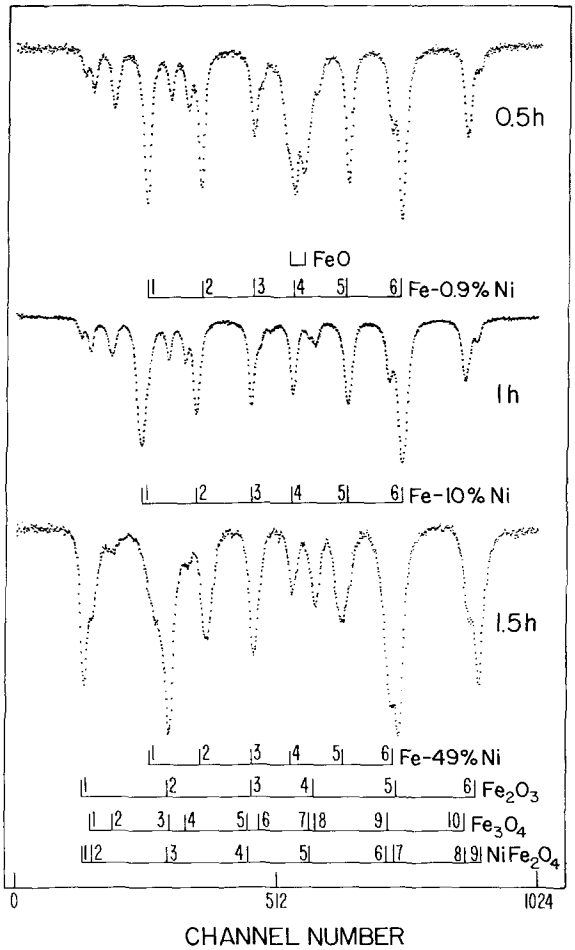

Figure 10 Room-temperature transmission Mössbauer spectra of $\approx 28\,\mu m$ thick samples of Fe–0.9% Ni, Fe–10% Ni and Fe–49% Ni alloys oxidized at 635° C for the times indicated.

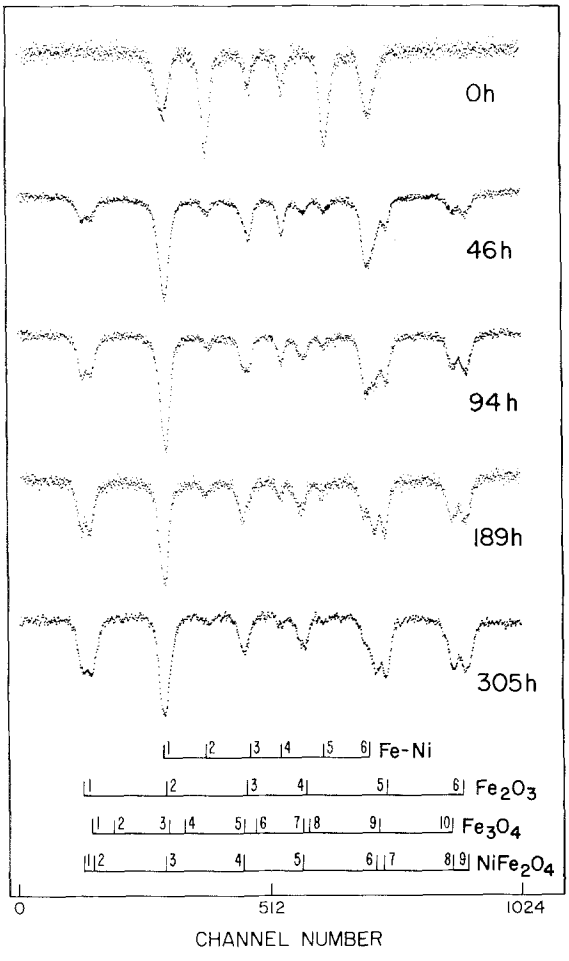

Figure 11 Room-temperature transmission Mössbauer spectra of $\approx 28\,\mu m$ thick samples of Fe–83% Ni alloy oxidized at 635° C for the times indicated.

hematite is a minor or major phase and whether the spinel is magnetite (or essentially so) or contains appreciable Ni, are as observed for the oxidations at 535° C. Furthermore, the Ni-containing spinel produced on the 49% Ni alloy seemed to be of very similar composition to that formed at the lower temperature. In the three alloy samples, a check by metallography was also made with respect to possible NiO formation at 635° C. None was detected in any cross-sections examined, i.e. as found for the 535° C oxidations. The sections of the oxidized 0.9% Ni alloy showed the "FeO" to be a separate layer in contact with the metal.

The spectra for the 83% Ni alloy oxidized at 635° C, shown in Fig. 11, are simpler than those determined for the previous alloys in the sense that the oxide contribution is almost entirely

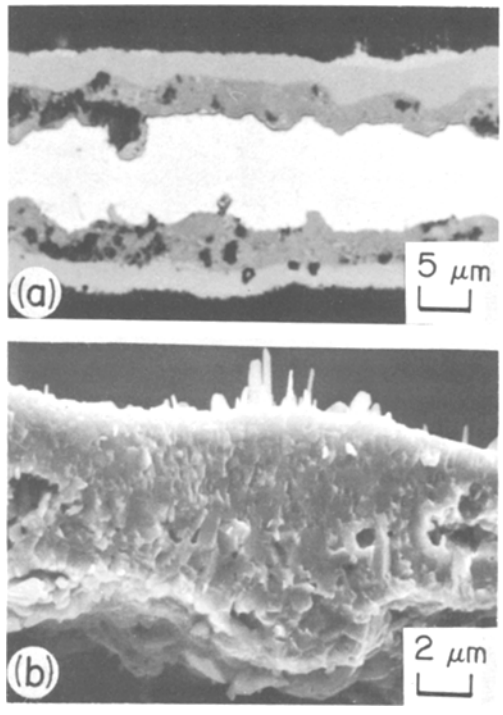

Figure 12 Metallographic and SEM sections of the Fe–83% Ni sample oxidized at 635° C for 94 h. (b) is of the oxide only. The oxide comprises roughly equal amounts of NiO (next to the alloy) and $NiFe_2O_4$, with a thin outer layer of α-Fe_2O_3.

attributable to $NiFe_2O_4$ (or oxide close to this composition) for all oxidation times. Comparison of the relative intensities of the first two (partially resolved) peaks due to the oxide with those of peaks 1 and 2 of $NiFe_2O_4$ (see Fig. 1) suggests the presence of a small amount of α-Fe_2O_3. The spectral lines due to the fcc alloy show slightly less splitting after oxidation of the alloy, but the effect, not surprisingly in view of the very high initial Ni content, is much less discernible than with the 49% Ni alloy.

Metallographic and SEM sections for the 83% Ni samples oxidized at 635° C from 46 to 305 h confirmed the presence of a fine layer of α-Fe_2O_3 covering the spinel. They also showed, in contrast with our observations on the less-rich Ni alloys, the formation of NiO which was a major oxide of thickness comparable with that of the spinel. Typical sections are shown in Fig. 12.

5. Discussion

The observed oxide phases are now discussed and also compared with previous oxidation data on Fe–Ni alloys of similar compositions at both

moderate and high temperatures. While no attempt was made in this research to gain information on the kinetics of oxide growth, it was noted, nevertheless, that the rate of scale growth on the alloys roughly obeyed a parabolic law. Accordingly, we shall refer to a rate constant K obtained using the equation $K = W^2/t$; W is the sample's oxygen uptake, derived either from intensity analysis of Mössbauer spectra to yield the approximate fraction of total Fe present as oxide [3], or from oxide thickness values determined by metallography, and t is the oxidation time. (Good correlation was noted between the two methods of evaluating K.)

5.1. 0.9% Ni alloy

It was evident that 0.9% Ni had little or no influence on the oxide phases produced during the oxidation of iron at 535° C. In addition, the relative proportions of α-Fe_2O_3 and Fe_3O_4, the two oxides occurring, were similar to those found in our earlier Mössbauer work [3] on the oxidation of pure iron foils in oxygen at comparable stages.

The overall oxidation rate was also similar. Intensity analysis of the 2, 8, and 32 h spectra of Fig. 3 led to an average value for K at 535° C of $\approx 1 \times 10^{-10}$ g^2 cm^{-4} sec^{-1}. This falls within the spread of parabolic rate constant values summarized by Caplan and Cohen [19] for the oxidation of unannealed iron in air and oxygen.

At 635° C, we observed a substantial FeO layer in addition to Fe_3O_4 and α-Fe_2O_3, i.e. as generally found for the oxidation of pure iron at temperatures $> 570°$ C. Similar three-layer scales have also been reported by Carter *et al.* [20, 21] for the oxidation of a 1% Ni alloy in oxygen at 1000° C. They found the oxidation rate to be lower, however, than for pure iron oxidation and this was associated with a lower proportion of FeO in the scale on the alloy.

5.2. 10% Ni alloy

Although the oxide phases observed following the oxidation of the 10% Ni alloy at 535° C did not seem to differ from those found after oxidation of the 0.9% Ni alloy, careful examination of the two series of spectra in Figs. 3 and 5 does indicate that the relative amount of α-Fe_2O_3 in the scale tended to be greater for the richer Ni alloy. For example, after 32 h oxidation of the 0.9% Ni alloy, when $\approx 30\%$ of the total Fe in the sample had still to be oxidized, the α-Fe_2O_3 component was $\approx 1/9$ of the scale. By contrast, after 73 h oxidation of the 10% Ni alloy, when a similar proportion of the Fe in the sample was unoxidized, the α-Fe_2O_3 represented $\approx 1/3$ of the scale.

As to the overall oxidation rate, this was less than observed for the 0.9% Ni alloy. The average value of K at 535° C derived from the 6, 17, 50 and 73 h spectra of Fig. 5 is about a factor of 2 lower at $\approx 4 \times 10^{-11}$ g^2 cm^{-4} sec^{-1}.

The lower oxidation rate and the somewhat greater proportion of α-Fe_2O_3 in the scale on the 10% Ni alloy was probably due to a reduced outward flux of Fe through the Fe_3O_4 as a consequence of a diminished supply of Fe to the alloy/oxide interface. This proposal is supported by the observation of a ragged interface (Fig. 6). According to Wagner's theory of the oxidation of an alloy containing a noble (or relatively noble) metal [22], such a morphology can arise when mass transport is controlled by diffusion in the alloy. Indeed, diffusion coefficients obtained by extrapolation of high-temperature data lead us to expect that diffusion in the alloy is much slower than diffusion in the Fe_3O_4 [23, 24]. Further support is provided by our Mössbauer measurements which suggest that strong Ni enrichment of the alloy occurred at the alloy/oxide interface (Section 4.2).

Magnetite and hematite were also the only oxides observed in the scale produced at 635° C. Evidently, there was a sufficiently high Ni concentration at the alloy/oxide interface, following the selective oxidation of Fe, to prevent the formation of FeO. The suppression of FeO is an effect that others have reported for Fe–Ni alloys, apart for those of very low Ni content [5, 21].

In earlier work, Gulbransen *et al.* [25] used reflection and transmission electron diffraction methods to study, respectively, the outer surface layers and main body of a thin oxide formed in oxygen at 300° C on a 4.9% Ni alloy. On the surface, they observed α-Fe_2O_3 and a spinel with lattice parameter $a = 8.43$ Å, while the main body of the oxide was a spinel with $a = 8.34$ Å. Although uncertainties in the interpretation of the spinel lattice parameters were not sufficiently low to make definite assignments, the surface spinel appeared to be Fe_3O_4, while the body of the oxide appeared to contain substantial Ni, perhaps corresponding to $NiFe_2O_4$*. Such an assignment

*a-values given by the ASTM X-ray diffraction file are 8.396 Å for Fe_3O_4 and 8.339 Å for $NiFe_2O_4$.

for the bulk of the spinel would, of course, contrast sharply with the present results at 535 and 635° C for the 10% Ni alloy which showed the spinel to be essentially Fe_3O_4 (average Ni content $\lesssim 3\%$ of the cations).

Incorporation of Ni into the spinel phase on alloys oxidized at high temperatures has been observed using electron probe techniques. Menzies and Lubkiewicz [26] have thus oxidized a 12% Ni alloy in oxygen and found that, at 700° C, α-Fe_2O_3 and Fe_3O_4 remained the only oxides in the scale until Ni enrichment of the underlying alloy surface reached 50 to 60% Ni. At this point, appreciable Ni entered the spinel phase eventually leading to the formation of $Ni_xFe_{3-x}O_4$ with $x \approx 0.24$ close to the alloy and <0.01 close to the α-Fe_2O_3. With increasing temperature (up to 1000° C), Ni entered the spinel early in the oxidation process and x values up to ≈ 0.4 were reported for the oxide next to the alloy/spinel interface. After oxidizing 5 to 20% Ni alloys in oxygen at 1000° C, Wulf *et al.* [21] have also found Ni in the spinel; the amount increased with increasing Ni content of the alloy with the spinel containing up to 10 to 15% Ni at the spinel/alloy interface on the 20% Ni alloy.

5.3. 49% Ni alloy

In marked contrast to the oxidation of the 0.9% and 10% Ni alloys at 535° C, we detected considerable amounts of Ni entering the Fe_3O_4 lattice and the oxide scale comprised roughly equal thicknesses of Fe–Ni spinel and α-Fe_2O_3. The average composition of the spinel derived from the Mössbauer spectra was $Ni_{0.5}Fe_{2.5}O_4$.

The overall oxidation rate of the 49% Ni alloy was substantially lower than that of the less-rich Ni alloys. Thickness measurements on metallographic sections of the samples oxidized for periods up to 88 h led to an average K value at 535° C of $\approx 1 \times 10^{-11}$ g^2 cm^{-4} sec^{-1}, an order of magnitude lower than found for the 0.9% Ni alloy. The continued decrease in oxidation rate relative to the 0.9% and 10% Ni alloys can probably be attributed to both slower diffusion in the alloy and to the presence of Ni in the spinel. The diffusion rate of Fe through the Ni-containing spinel has been reported to be much lower than through Fe_3O_4 [27]. The increased proportion of α-Fe_2O_3 in the scale would also follow from a reduced outward flux of Fe through the spinel.

*This alloy contained additionally 2% Mn.

The earlier reflection and transmission electron diffraction studies of Gulbransen *et al.* [25] on the oxide formed on a 4.9% Ni alloy were applied also to a 49% Ni alloy*. Following oxidation of the alloy in oxygen at 300° C, they found α-Fe_2O_3 and a spinel with $a = 8.42$ Å close to the surface of the oxide, and by transmission they observed α-Fe_2O_3, a spinel with $a = 8.34$ Å and NiO. Again, it appeared that the surface spinel was probably Fe_3O_4, while the bulk of the spinel probably contained substantial Ni.

Reflection electron diffraction measurements were also reported by Foley *et al.* [28] on the oxide produced on a 42% Ni alloy in air at 600 to 900° C. Hematite and ferrite were observed and it was postulated that the latter was closer to $NiFe_2O_4$ than to Fe_3O_4, because the measured lattice parameter was 8.33 Å and chemical analysis indicated high Ni concentrations in the oxide.

Scales consisting of roughly equally thick layers of α-Fe_2O_3 and Fe–Ni spinel similar to those presently seen at 535 and 635° C have been recorded in other studies at temperatures up to 1000° C. Thus, Menzies and Lubkiewicz [29] have oxidized a 30% Ni alloy at 700 to 1000° C in oxygen and reported α-Fe_2O_3 and $Ni_xFe_{3-x}O_4$ with x, assessed from electron probe microanalysis, reaching values >0.5. Kennedy *et al.* [30] reported the scale on a 26% Ni alloy oxidized in oxygen at 800° C to be α-Fe_2O_3 and $Ni_xFe_{3-x}O_4$ (with traces of FeO and NiO adjacent to the alloy), and in this case precise X-ray diffraction lattice parameter measurements indicated x to be ≈ 0.4.

Wulf *et al.* [21], after oxidizing a 50% Ni alloy in oxygen at 1000° C, also observed a Ni-containing spinel (20% Ni). The scale was, however, of quite different overall structure from those observed by Menzies and Lubkiewicz [29] and Kennedy *et al.* [30]; it contained a layer of NiO next to the alloy and the α-Fe_2O_3 was present on the spinel, the predominant phase, in the form of isolated islands.

It is apparent that a feature of the oxidation of fairly rich Ni alloys at both moderate and high temperatures is the formation of a spinel which contains substantial Ni.

5.4. 83% Ni alloy

The spinel phase produced on oxidation of the 83% Ni alloy at 635° C had a composition of, or very close to, $NiFe_2O_4$. A thin outer covering of

α-Fe_2O_3 was part of the scale and for this alloy, in contrast to the less-rich Ni alloys investigated, a major oxide phase next to the alloy was NiO.

Previous electron diffraction studies [31] on an 80% Ni alloy oxidized in air at 700 and 900° C indicated that a spinel, apparently closer to $NiFe_2O_4$ than to Fe_3O_4, formed initially. It is evident that, in our experiments, the Ni enrichment of the alloy beneath the scale was sufficient for the formation of NiO which occupied $\approx 50\%$ of the scale.

Scales in which $\approx 50\%$ of the thickness is taken up by NiO have also been reported by Kennedy *et al.* [30] on 75% and 84% Ni alloys oxidized in oxygen at 800° C and by Dalvi and Smeltzer [32] on 75 to 85% Ni alloys oxidized in oxygen at 1000° C. In both works the spinel was rich in Ni, and in one case [30] α-Fe_2O_3 was also present as a thin outer layer while in the other [32] no α-Fe_2O_3 was reported.

Metallographic work in our preliminary experiments on the 83% Ni alloy at 535° C led to a K value of $\sim 2 \times 10^{-13}$ g^2 cm^{-4} sec^{-1} and at 635° C, K increased to $\sim 3 \times 10^{-12}$ g^2 cm^{-4} sec^{-1}. The oxidation rate is thus much lower than observed for the less-rich Ni alloys and it approximates that of cold-worked pure nickel [33]. NiO forms on this alloy as a result of the high Ni activity at the interface. The oxidation rate is lower because of NiO formation and growth, and the growth of the nickel ferrite is slower than on the 49% Ni alloy because of the reduced activity gradient across the ferrite.

6. Conclusions

Supported by other techniques, Fe^{57} transmission Mössbauer spectroscopy has proved useful for studying the oxidation of Fe–Ni alloys in 1 atm. air at 535° C and 635° C. With increasing Ni content of the alloy, the composition of the scale changed and the oxidation rate decreased. The essential results for the 4 alloys examined are as follows:

(1) 0.9% Ni alloy; the scale produced at 535° C was Fe_3O_4 covered by a thin outer layer of α-Fe_2O_3 and the oxidation rate (parabolic rate constant, K, $\approx 1 \times 10^{-10}$ g^2 cm^{-4} sec^{-1}) was similar to that of pure iron. FeO formed additionally at 635° C as a major phase next to the alloy.

(2) 10% Ni alloy; at both 535 and 635° C, the scale consisted of Fe_3O_4 (Ni content $\leqslant 3\%$ of the cations) and α-Fe_2O_3. It was similar to the scale produced at 535° C on the 0.9% Ni alloy, although the thin α-Fe_2O_3 layer tended to be relatively thicker. The oxidation rate at 535° C was a factor of ~ 2 lower than observed for the 0.9% Ni alloy.

(3) 49% Ni alloy; the scale at both 535 and 635° C consisted of an inner layer of $Ni_xFe_{3-x}O_4$ (with $x \approx 0.5$, on average) and an outer layer, of similar thickness, of α-Fe_2O_3. The oxidation rate at 535° C was a factor of ~ 10 lower than found for the 0.9% Ni alloy.

(4) 83% Ni alloy; at 635° C, the scale comprised roughly equally thick layers of NiO (next to the alloy) and $NiFe_2O_4$, and a thin outer covering of α-Fe_2O_3. The oxidation rate at 535° C was a factor of ~ 500 lower than for the 0.9% Ni alloy.

Acknowledgement

This work took place while one of us (DAC) was a Visiting Scientist firstly in the Spectroscopy Group at BNL and subsequently in the Metallic Corrosion and Oxidation Group at NRCC. This author wishes to thank the respective heads of the two groups, Dr G. C. Allen and Dr M. Cohen, for making these visits possible and also for the warm hospitality extended to him. We are indebted to the following technical staff at NRCC: G. I. Sproule for SEM examinations, P. E. Beaubien for metallographic work and Mrs F. Lee for X-ray diffraction analyses. This paper is published by permission of the CEGB and is NRCC No. 15852.

References

1. D. A. CHANNING and M. J. GRAHAM, CEGB Report RD/B/N1384 (1969).
2. *Idem, J. Electrochem. Soc.* **117** (1970) 389.
3. *Idem, Corrosion Sci.* **12** (1972) 271.
4. D. A. CHANNING, M. J. GRAHAM and S. M. DICKERSON, *ibid* **13** (1973) 933.
5. R. T. FOLEY, *J. Electrochem. Soc.* **109** (1962) 1202.
6. O. C. KISTNER and A. W. SUNYAR, *Phys. Rev. Letters* **4** (1960) 412.
7. F. VAN DER WOUDE, *Phys. Stat. Sol.* **17** (1966) 417.
8. R. BAUMINGER, S. G. COHEN, A. MARINOV, S. OFER and E. SEGAL, *Phys. Rev.* **122** (1961) 1447.
9. J. M. D. COEY, A. H. MORRISH and G. A. SAWATZKY, *J. de Physique,* **32** (1971) C1-271.
10. I. BUNGET, C. NISTOR and M. ROSENBERG, *ibid* **32** (1971) C1-274.
11. B. J. EVANS, *Amer. Inst. Phys. Conf. Proc.* **10** (1973) 1398.
12. G. A. SAWATZKY, F. VAN DER WOUDE and A. H. MORRISH, *Phys. Rev.* **183** (1969) 383.

13. J. W. LINNETT and M. M. RAHMAN, *J. Phys. Chem. Sol.* **33** (1972) 1465.
14. J. P. MOREL, *ibid* **28** (1967) 629.
15. M. HANSEN, "Constitution of Binary Alloys", (McGraw Hill, New York, 1958) p. 677.
16. C. E. JOHNSON, M. S. RIDOUT and T. E. CRANSHAW, *Proc. Phys. Soc.* **81** (1963) 1079.
17. R. S. PRESTON, S. S. HANNA and J. HERBERLE, *Phys. Rev.* **128** (1962) 2207.
18. N. N. GREENWOOD and A. T. HOWE, *J. Chem. Soc. Dalton Trans.* **1** (1972) 110.
19. D. CAPLAN and M. COHEN, *Corrosion Sci.* **6** (1966) 321.
20. T. J. CARTER, G. L. WULF and G. R. WALLWORK, *ibid* **9** (1969) 471.
21. G. L. WULF, T. J. CARTER and G. R. WALLWORK, *ibid* **9** (1969) 689.
22. C. WAGNER, *J. Electrochem. Soc.* **103** (1956) 571.
23. C. J. SMITHELLS, "Metals Reference Book", Vol. 2, 4th Edition (Butterworth, London, and Plenum Press, New York, 1967) p.658.
24. L. HIMMEL, R. F. MEHL and C. E. BIRCHENALL, *Trans. AIME* **197** (1953) 827.
25. E. A. GULBRANSEN, R. T. PHELPS and J. HICKMAN, *Ind. Eng. Chem.* (Anal. Ed.) **18** (194 640.
26. I. A. MENZIES and J. LUBKIEWICZ, *Oxid. of met* 3 (1971) 41.
27. R. H. CONDIT, M. J. BRABERS and C. BIRCHENALL, *Trans. AIME* **218** (1960) 768.
28. R. T. FOLEY, J. U. DRUCK and R. E. FRYXEL *J. Electrochem. Soc.* **102** (1955) 440.
29. I. A. MENZIES and J. LUBKIEWICZ, *ibid* **1** (1970) 1539.
30. S. W. KENNEDY, L. D. CALVERT and M. COHE *Trans. AIME* **215** (1959) 64.
31. R. T. FOLEY, *J. Electrochem. Soc.* **108** (1961) 21
32. A. D. DALVI and W. W. SMELTZER, *ibid* **1** (1971) 1978.
33. D. CAPLAN, M. J. GRAHAM and M. COHEN, *ib* **119** (1972) 1205.

Received 7 March and accepted 4 April 1977.